



Published in final edited form as:

*J Chromatogr B Analyt Technol Biomed Life Sci.* 2009 September 15; 877(26): 2755–2767. doi:10.1016/j.jchromb.2009.01.008.

## Lipidomic analysis of endocannabinoid metabolism in biological samples

Giuseppe Astarita and Daniele Piomelli

Department of Pharmacology, University of California, Irvine, CA 92967

### Abstract

The endocannabinoids are signaling lipids present in many living organisms. They activate G protein-coupled cannabinoid receptors to modulate a broad range of biological processes that include emotion, cognition, inflammation and reproduction. The endocannabinoids are embedded in an interconnected network of cellular lipid pathways, the regulation of which is likely to control the strength and duration of endocannabinoid signals. Therefore, physiopathological or pharmacological perturbations of these pathways may indirectly affect endocannabinoid activity and, *vice versa*, endocannabinoid activity may influence lipid pathways involved in other metabolic and signaling events. Recent progress in liquid chromatography and mass spectrometry has fueled the development of targeted lipidomic approaches, which allow researchers to examine complex lipid interactions in cells and gain a broader view of the endocannabinoid system. Here, we review these new developments from the perspective of our laboratory's experience in the field.

### Keywords

lipidomics; anandamide; 2-arachidonoylglycerol (2-AG); N-acyl phosphatidylethanolamine (NAPE); fatty acid amide hydrolase (FAAH); diacylglycerol (DAG); triacylglycerol (TAG); arachidonic acid; prostaglandin

## 1. Introduction

The endocannabinoid signaling system is part of a network of cellular lipid pathways. Perturbations of such pathways, induced by physiological or pathological events, may strongly affect endocannabinoid function. Recent advances liquid chromatography (LC) and mass spectrometry (MS) have fueled the development of lipidomics, a branch of metabolomics that has enormous potential for the study of endocannabinoid metabolism. Indeed, lipidomic approaches can be combined with genetic and pharmacological strategies to address many unsolved questions on the roles and regulation of endocannabinoid signaling. Considerable progress has been made in understanding the physiological and pathological roles of endocannabinoids and several recent reviews discuss these topics in detail [1,2]. Here, we will focus on recent advances in the development and application of lipidomics to the study of the endocannabinoid system.

---

Correspondence to: Daniele Piomelli, PhD, Department of Pharmacology, University of California, Irvine; Irvine, CA 92697-4625; Phone: (949) 824-6180; Fax: (949) 824-6305; E-mail: piomelli@uci.edu.

**Publisher's Disclaimer:** This is a PDF file of an unedited manuscript that has been accepted for publication. As a service to our customers we are providing this early version of the manuscript. The manuscript will undergo copyediting, typesetting, and review of the resulting proof before it is published in its final citable form. Please note that during the production process errors may be discovered which could affect the content, and all legal disclaimers that apply to the journal pertain.

### 1.1. Endocannabinoid metabolism: a complex picture

The endocannabinoids are endogenous lipids derived from polyunsaturated fatty acids. The two best known endocannabinoids, arachidonylethanolamide (anandamide) and 2-arachidonoyl-*sn*-glycerol (2-AG), are both derivatives of arachidonic acid. These molecules are found in all mammalian tissues and provide a classic example of signaling lipids. They are produced by cells on demand and bind to G protein-coupled receptors, called cannabinoid receptors, which mediate their action. Cannabinoid receptors participate in the regulation of many physiological processes, such as emotion, reward, cognition, inflammation and reproduction. In the last two decades, much research has been devoted to studying the formation and deactivation of individual endocannabinoid lipids in mammalian tissues, with the intent of elucidating their biological regulation. These analyses have initially relied on techniques such as thin-layer chromatography (TLC) and gas chromatography-mass spectrometry (GC/MS). Recent progress in LC/MS has greatly facilitated these efforts, allowing researchers to place individual endocannabinoid molecules in the context of the interconnected network of their substrates and products. Indeed, not only are the endocannabinoids produced through biochemical pathways that yield a sequence of functionally distinct signaling lipids, but also different biochemical pathways are used to generate the same endocannabinoid molecule [3]. Thus, the same enzymes and lipid substrates can be often shared between endocannabinoid and other metabolic pathways. The development of analytical approaches that consider the ensemble of the endocannabinoid system, rather than its individual components in isolation, could be invaluable to elucidate the physiopathological roles of this signaling system.

### 1.2. LC/MS of endocannabinoids

The beginning of the endocannabinoid field was marked by the discovery in 1992 of the first endogenous cannabinoid receptor ligand, the fatty acid ethanolamide anandamide [4]. Initially, endocannabinoids analysis relied heavily on TLC, LC and GC/MS [5-7]. However, these techniques often require multiple analytical steps, including chemical derivatization and serial enzymatic hydrolysis, which render analyses very laborious and time-consuming. The advent of LC/MS has completely changed this scenario. Using LC/MS we can identify and quantify individual endocannabinoid molecules in a single step using analytical platforms, such as tandem mass spectrometry (MS/MS), which provide the detailed structural information necessary for the characterization of lipids in complex biological matrices [8]. Furthermore, the invention of ionization techniques such as electrospray ionization (ESI) and atmospheric pressure chemical ionization (APCI), which permit the direct coupling of LC to MS, has allowed researchers to identify and quantify the endocannabinoids with greater sensitivity than ever before possible [9-13]. Therefore, the combination of LC and MS has emerged as the technique of choice for endocannabinoid analyses.

### 1.3 Lipidomics to study endocannabinoid metabolism

Many aspects of endocannabinoid metabolism are still incompletely understood. For example, it is unclear how changes in endocannabinoid signaling affect distal lipid pathways, and, *vice versa*, how alterations in cellular lipid metabolism influence endocannabinoid signaling. In addition, we do not understand the specific contributions of each of the biosynthetic and degradative enzymes that have been identified in endocannabinoid metabolism. Lipidomics can help answer these questions by offering a large-scale view of lipid alterations accompanying perturbations of endocannabinoid metabolism. For example, the analysis of lipid profiles associated with genetic or pharmacological manipulations of the endocannabinoid system might shed new light on the biochemical mechanisms underlying the regulation of endocannabinoid metabolism [12,14,15]. Furthermore, lipidomic information can be integrated into multidisciplinary datasets deriving from genomics, transcriptomics and

proteomics. Such a system biology approach would offer novel insights on the effects of genetic or protein diversity on endocannabinoid metabolism.

In the following sections, we illustrate the development and application of a comprehensive lipidomic approach to study endocannabinoid metabolism in biological samples.

## 2. Lipidomic analysis of endocannabinoids and related lipids

The endocannabinoid system is constituted of three major lipid classes: glycerophospholipids, glycerolipids and fatty acyls. Because these lipids have a wide variety of chemical structures and dynamic range of concentrations, several approaches have been developed for their analysis [12,16-18]. A large-scale LC/MS lipidomic strategy for the identification and quantification of various classes of lipids in biological samples is presented in Fig. 1. Such strategy requires the combination of three analytical steps: 1) sample preparation by organic solvent extraction and lipid fractionation by open-bed silica-gel chromatography, which separates low-abundance lipids from molecules that might interfere or suppress their detection; 2) chromatographic separation using two different octadecyl (C18) reversed-phase LC columns, which can fractionate lipids based on their size, number of double bonds and diffusion properties; and 3) intrasource-ionization separation coupled to MS in either the positive or negative mode, which differentiates lipids based on their ionization properties.

### 2.1. Step 1. Sample preparation

**2.1.1. Lipid extraction**—Sample preparation includes lipid extraction from the biological matrix and removal of most non-lipid contaminants from the extract. Usually, lipid concentrations in biological samples are normalized by tissue weight or protein, total phospholipid or DNA concentration. Absolute quantification is made possible by using non-endogenous structural analogs (internal standards), which are added before the extraction procedure. A variety of mixtures of organic solvents have been utilized to extract lipid classes from biological samples [19-25]. The modified Folch procedure for lipid extraction utilized in our laboratory allows for greater than 90% recovery of most lipids [26]. In such procedure, snap-frozen tissues are weighed and homogenized in ice-cold methanol (1 ml per 100 mg tissue) to quench any possible enzymatic reaction that might interfere with the analysis. The methanol contains appropriate internal standards (*see next section*), which also act as carriers to reduce analyte loss during sample work-up. Samples from the homogenates are taken for protein measurements. Lipids are extracted with chloroform (2 vol) and washed with water (0.75 vol). Organic phases are collected and dried under a stream of N<sub>2</sub> (important to prevent lipid oxidation). Alternative extraction methods are recommended for the quantitative isolation of acidic phospholipids such as phosphoinositides [18,27].

**2.1.2. Internal standards**—Quantitation of lipid species in biological samples can be achieved by normalizing the individual molecular ion peak intensity with an internal standard for each lipid class. A mixture of non-endogenous molecules can be used as internal standards, which allow lipid levels to be normalized for both extraction efficiency and instrument response. A representative list of commercially available internal standards for each lipid class includes the following chemicals: 1) fatty-acid ethanolamides: deuterated and non-deuterated fatty acid ethanolamides can be synthesized as previously reported [12] or purchased from commercial sources such as Cayman Chemicals (Ann Arbor, MI, USA); 2) fatty acids: heptadecanoic acid from Nu-Chek Prep (Elysian, MN, USA) or d<sub>8</sub>-arachidonic acid (Cayman Chemicals); 3) *N*-acyl-phosphatidylethanolamine: 1,2-dipalmitoyl-*sn*-glycero-3-phosphoethanolamine-*N*-heptadecanoyl can be synthesized as previously described [12]; alternatively 1-O-hexadecyl-2-palmitoyl-*sn*-glycero-3-phosphoethanolamine-*N*-palmitoyl may be purchased from Sigma-Aldrich (St. Louis, MI, USA); 4) oxygenated

endocannabinoids:  $d_4$ -PGF<sub>2α</sub> ethanolamide and prostaglandin:  $d_4$ -prostaglandin-E<sub>2</sub> (Cayman Chemicals); 5) triacylglycerol: trionadecenoin from Nu-Chek Prep; 6) diacylglycerol: dinodadienoin (Nu-Chek Prep); 7) monoacylglycerol: monoheptadecanoin (Nu-Chek Prep) or  $d_8$ -2-arachidonoyl-*sn*-glycerol (Cayman Chemicals); 8) phosphatidylethanolamine: 1,2-diheptadecanoyl-*sn*-glycero-3-phosphoethanolamine (Avanti Polar Lipids; Alabaster, AL, USA); 9) phosphatidylcholine: 1,2-diheptadecanoyl-*sn*-glycero-3-phosphocholine (Avanti); 10) phosphatidylinositol: 1,2-dipalmitoyl-*sn*-glycero-3-phosphoinositol (Avanti).

**2.1.3. Lipid fractionation**—Various solid-phase extraction chromatography procedures have been used to fractionate lipid classes. The standardized extraction procedure employed in our lab is illustrated in Fig. 1. After solvent extraction, the organic phase is divided into two parts. The first is directly analyzed by LC/MS<sup>n</sup> to measure high-abundance, positively charged lipids (e.g., phosphatidylcholines). The second part is fractionated by open-bed silica gel column chromatography (Silica gel 60 230-400 mesh) prior to LC/MS<sup>n</sup> analyses. A serial elution with 9:1 and 1:1 chloroform/methanol (vol:vol) is used to separate lipid groups according to their relative polarities (Fig. 1).

## 2.2. Step 2. Chromatographic separation

Reversed-phase LC can be used to separate lipids based on to their fatty acyl chain length and degree of unsaturation. Lipids species containing longer acyl chains elute from the LC column later than do shorter-chain lipids (e.g. C18:0>C16:0>C14:0), while saturated acyl structures tend to elute later than do long polyunsaturated ones (e.g. C18:0>C18:1>C18:2). Generally, the first double bond on an acyl chain reduces the effective chain length by a little less than 2 carbon units, while additional double bonds have smaller effects on retention. The combinatorial nature of complex lipids makes possible only a partial separation of isomeric species. Therefore, to further characterize samples containing such lipids, LC separation is coupled with MS<sup>n</sup>, which allows each lipid species to be identified based on both retention time and MS<sup>n</sup> properties (Fig. 1).

**2.2.1. Analysis of small lipids**—Small lipids, which we define here as molecules containing a single fatty acyl group, can be separated using a reversed-phase C18 LC column packed with conventional porous silica particles of small diameter (Fig. 1). For small neutral lipids (e.g. esters and amides of fatty acids), a linear gradient of methanol (or acetonitrile) in water is used. More polar small lipids (e.g. fatty acids and their derivatives containing a free carboxylic group or lysophospholipids containing a phosphate group) can be separated using a linear gradient of methanol in water containing acetate buffer (5 mM ammonium acetate, 0.25% acetic acid, pH 3.8), which is included to improve peak shape. These reversed-phase LC conditions generally allow for the separation of small lipids that differ in double bond number and/or chain length.

**2.2.2. Analysis of large apolar, anionic and cationic lipids**—Large lipids, defined here as molecules containing two or more fatty acyl groups, may be separated using a reversed-phase C18 LC column packed with superficially porous particles (e.g., SB300 Poroshell column, Agilent-Technologies, CA, USA) (Fig. 1). A linear gradient of methanol (or acetonitrile) in water containing acetate buffer affords good peak shape at fast flow rates. This is probably due to the fact that large lipids rapidly penetrate the thin shell of the superficial coating material, reducing diffusion and peak tailing. A combination of high temperature and high flow velocities improves the separation speed, resulting in better peak shape.

## 2.3. Step 3. Intrasource ionization coupled to MS separation of lipid molecules

Most lipids can be detected using either ESI or APCI techniques. Here, we illustrate an approach that uses ESI in either the positive or negative mode (Fig. 1).

**2.3.1. Small lipids**—Small neutral lipids (e.g. esters or amides of fatty acids) are generally detected as protonated molecular ions or sodium and ammonium adducts in the positive ESI mode. In contrast, more polar small lipids (e.g. those containing free carboxylic or phosphate groups) are detected as deprotonated molecular ions in the negative ESI mode (Fig. 1).

**2.3.2. Large lipids**—Large apolar lipids (e.g., triacylglycerols, TAGs, and diacylglycerols, DAGs) are detected as sodium or ammonium adducts in the positive ESI mode. Large lipids containing a positively charged group (e.g. phosphatidylcholine), can be detected as positively charged molecular ions in the positive ESI mode. Alternatively, such lipids can be also detected as acetate adducts in the negative ESI mode. In contrast, large anionic lipids are detected as deprotonated molecular ions in the negative ESI mode (Fig. 1).

## 2.4. LC/MS tools for metabolite discovery

**2.4.1. LC/MS imaging**—Traditional ways to represent LC/MS runs (peak intensity vs retention time) (Fig. 2A, top) provide limited information, owing to the coexistence in a single sample of multiple isobaric and isomeric molecular species. A practical solution to bypass this problem is to represent LC/MS chromatograms as 3D maps (LC elution time vs mass vs intensity) (Fig. 2A, bottom) [12,14]. This imaging tool allows for an intuitive visual inspection of the molecular content of a biological sample and can also be used for qualitative analysis [12,14].

**2.4.2. Gentle ESI/MS<sup>n</sup> fragmentation**—The combination of soft ionization techniques such as ESI and the gentle process of fragmentation produced by the ion trap instrument generates a series of fragment ions that may be found physiologically as neutral molecular species (Fig. 2B). For example, fragments generated by the ESI/MS<sup>n</sup> analysis of complex lipid species are also common products of enzymatic hydrolysis (e.g., lysophospholipids and fatty acids) or chemical rearrangement (e.g., products of intramolecular cyclization of phosphate groups) (Fig.2B) [12]. This suggests that a “gentle fragmentation approach” can be used as a discovery tool in biochemistry for the study of catabolic products of known biomolecules and the identification of novel biologically relevant metabolites.

## 3. Metabolism of anandamide

Anandamide is biosynthesized through cleavage of a group of membrane glycerophospholipid precursors in response to extracellular signals (Fig. 3). In the next section, we illustrate the applications of a lipidomic approach (previously described in *Section 2*) to the analysis of anandamide formation and degradation in human brain samples (frontal cortex from healthy male subjects aging from 64 to 82; average post mortem interval 4.2 hours) obtained through the courtesy of Drs. Carl W. Cotman and Dr. Elizabeth Head (Institute for Brain Aging and Dementia and Alzheimer’s Disease Research Center at University of California, Irvine).

### 3.1. Lipid remodeling of anandamide precursors

A likely physiological route for the formation of anandamide requires the generation of *N*-arachidonoyl-phosphatidylethanolamines (NAPEs), which are produced through the transfer of arachidonic acid from the *sn*-1 position of phospholipids (e.g., phosphatidylcholine, PC) to the primary amine of phosphatidylethanolamine (PE, Fig. 4; method details are in the figure legend) [12,28-30]. This reaction is catalyzed by an as-yet-uncharacterized *N*-acyltransferase (NAT), which may also be involved in the biosynthesis of other *N*-acyl PE [12,28-30] (Fig. 3) (see *Section 3.5*). Figure 5 shows the LC/MS<sup>n</sup> identification of a NAPE precursor, 1,2-diarachidonoyl-phosphatidylcholine, in frozen human brain sample (method details are in the figure legend).

### 3.2. Anandamide formation

Starting from NAPEs (Fig. 6), three distinct biochemical pathways have been proposed for the formation of anandamide (Fig. 3): 1) the direct conversion of NAPE to anandamide by a NAPE-specific phospholipase D (PLD) [5,31]; 2) the hydrolysis of NAPE by a NAPE-specific phospholipase A1/A2 (e.g.  $\alpha/\beta$  hydrolase-4, ABHD-4) to form the intermediates lyso-NAPE (Fig. 6) and glycerophospho-anandamide, which are then cleaved by PLD [32-34]; 3) the hydrolysis of NAPE catalyzed by a NAPE-specific phospholipase C to yield the intermediate phosphoanandamide, which can then be cleaved by a lipid phosphatase such as protein tyrosine phosphatase, non-receptor type 22[35,36].

### 3.3. Anandamide degradation

Anandamide degradation requires first its transport across the plasma membrane, which may occur by carrier-mediated facilitated diffusion [37-39]. Once inside the cell, anandamide is hydrolyzed to arachidonic acid and ethanolamine by intracellular, membrane-bound fatty acid amide hydrolases (FAAHs) [40,41]. FAAHs also hydrolyze other bioactive fatty acid amides (e.g. fatty acid primary amides and *N*-acyl amino acids, see *Section 3.5*) [42-44].

### 3.4. Oxidative metabolism of anandamide

Anandamide can be metabolized by cyclooxygenase-2 (COX-2), 12- and 15-lipoxygenase (LOX), and cytochrome P450 (CYP450) to generate prostaglandin ethanolamides (prostamides), hydroperoxides, hydroxy and epoxide metabolites (Fig. 3) [45-52]. Most of these molecules have low affinity for cannabinoid receptors and display moderate activity as FAAH inhibitors, which may result in a potentiation of anandamide signaling. However, because of their extremely low concentrations in tissues, their physiological functions remain unclear.

### 3.5. Fatty-acid ethanolamides (FAEs)

Anandamide belongs to the fatty acid ethanolamide (FAEs) (or else *N*-acylethanolamides, NAEs) family of signaling lipids, which include both cannabimimetic and noncannabimimetic molecules that are present in most mammalian tissues. These molecules, which only differ in length and degree of unsaturation of their acyl chains, share several biosynthetic and degradative enzymes.

**3.5.1. Cannabimimetic FAEs**—Two polyunsaturated FAEs, docosatetraenoylethanolamide (C22:4,  $\Delta^{7-10-13-16}$ ) and dihomo- $\gamma$ -linolenylethanolamide (C20:3,  $\Delta^{8-11-14}$ ) bind with high affinity to cannabinoid receptors [53,54] and produce pharmacological effects similar to those of anandamide. Notably, our analyses show that these two lipids are present in human brain tissue at concentrations comparable to those of anandamide (Fig. 7).

**3.5.2. Non-cannabimimetic FAEs**—Most endogenous FAEs do not productively bind cannabinoid receptors [55]. Yet, their levels are from 1-10 times higher than those of anandamide and they may serve important physiological functions. For example, palmitoylethanolamide (C16:0) and oleoylethanolamide (C18:1,  $\Delta^9$ ) (Fig. 7) are endogenous ligands for the nuclear receptor peroxisome-activated receptor-alpha (PPAR-alpha) and exert anorexic, analgesic and antiinflammatory effects [56-60]. Stearoylethanolamide (C18:0) (Fig. 7) also appears to produce antiinflammatory and anorexic effects [61-63]. The biological distribution of other FAEs such as linoleoylethanolamide (C18:2,  $\Delta^{9-12}$ ) and linolenylethanolamide (C18:3,  $\Delta^{6-9-12}$ ) in rat appears to be tissue-specific, with very high levels in peripheral tissues (e.g., intestine) [14,64], while almost undetectable levels in the brain.

### 3.6. Fatty-acid amides

Besides FAEs, fatty acyl amide analogs of anandamide include two additional classes of endogenous molecules: 1) primary fatty acid amides (e.g. oleamide) [65]; 2) *N*-acyl amino acids (also called elmiric acids), which derive from the conjugation of fatty acids with amino acids or amino-acid derivatives (e.g. *N*-acyl glycine, *N*-acyl taurine, *N*-acyl serotonin and *N*-acyl dopamine) [55,66,67]. Although some of these amides have clear pharmacological effects, such as the activation of the TRPV-1 receptor channels, the elucidation of their physiological roles awaits further investigation. It is important to point out that several such amides (e.g., oleamide) are commonly used in the production of plasticware, and may thus leach into the biological samples during work-up [68].

### 3.7. Assays for the metabolism of anandamide

Several enzymatic assays have been developed to study anandamide metabolism *in vitro* [12, 14]. Here, we review some selected examples of assays relying on fast and ultra-fast LC/MS analysis.

**3.7.1. NAPE biosynthesis [12]**—The *N*-acylation of PE (e.g. by NAT activity) can be measured by incubating (at 37°C in 50mM Tris-HCl, pH 8.0 and 0.1% Triton X-100) a protein preparation and synthetic 1,2-diheptadecanoyl-*sn*-glycero-3-phosphoethanolamine, which is used as a substrate. The reaction product, 1,2-diheptadecanoyl-*sn*-glycero-3-phosphoethanolamine-*N*-arachidonoyl, can be measured by LC/MS using 1,2-dipalmitoyl-*sn*-glycero-3-phosphoethanolamine-*N*-heptadecanoyl as an internal standard.

**3.7.2. NAPE hydrolysis [14]**—The rate of NAPE hydrolysis (e.g. by NAPE-PLD activity) can be determined by incubating (at 37 °C in 50 mM Tris-HCl, pH 7.4 and 0.1% Triton X-100, 1 mM phenylmethylsulphonyl fluoride) a protein preparation in the presence of the synthetic 1,2-dipalmitoyl-*sn*-glycero-3-phosphoethanolamine-*N*-heptadecanoyl, which is used as substrate and can be synthesized as previously reported [12]. The final product, heptadecanoylethanolamide, can be monitored by LC/MS using d<sub>4</sub>-heptadecanoylethanolamide as an internal standard.

**3.7.3. Anandamide degradation**—Anandamide hydrolysis (e.g. by FAAH activity) can be measured by incubating (at 37°C in 50mM Tris-HCl, pH 8.0 and 0.05% fatty acid-free bovine serum albumin) a protein preparation in the presence of synthetic heptadecanoylethanolamide, which is used as substrate and can be synthesized as previously reported [14]. The final product, heptadecanoic acid (C17:0), can be monitored by LC/MS using heptadecenoic acid (C17:1, Δ<sup>10</sup>) as internal standard.

## 4. Metabolism of 2-AG

2-AG biosynthesis in neural cells is driven by a rise in intracellular calcium levels and/or activation of G<sub>q/11</sub>-coupled receptors [2,15,69], and proceeds through a series of pathways that are distinct from those involved in anandamide production (Fig. 8). In the following section, we review current applications for the lipidomic analysis of 2-AG metabolism in human brain samples (*Section 3*).

### 4.1. Lipid remodeling of 2-AG precursors

2-AG formation requires the generation of arachidonic acid-containing DAGs and lysoglycerophospholipid species (Fig. 8).

**4.1.1. DAGs**—DAGs can derive from three main enzymatic routes: 1) PLC-mediated hydrolysis of membrane phospholipids, particularly phosphoinositides; 2) phosphatase-

mediated hydrolysis of phosphatidic acid (PA); 3) lipase-mediated hydrolysis of TAGs (Fig. 8). The fatty acid compositions of DAGs formed by these various routes reflect the composition of the parent lipid. In particular, those derived from inositol phospholipids are highly enriched in molecular species containing stearic acid in position *sn*-1 and arachidonic acid in position *sn*-2 (Fig. 9A) [15]. However, also phosphatidylcholine (Fig. 9B) and PA may serve as source of 1-acyl,2-arachidonoyl-DAG [70-72]. Furthermore, our analysis reveal that several arachidonoyl-containing TAG species are present in human brain, which might contribute to DAG and 2-AG formation (Fig.10). The biological significance of neuronal TAGs is unclear at present. Finally, recent evidence suggests the existence of preformed DAG pools in neurons, which may be directly hydrolyzed to 2-AG in response to stimuli [15,73].

**4.1.2. Lysophospholipids**—Arachidonoyl-containing lysophospholipids may contribute to 2-AG formation [74]. Such lysophospholipids may derive from the PLA<sub>1</sub>-mediated hydrolysis of phospholipids (Fig. 8).

#### 4.2. 2-AG formation

Three biosynthetic pathways have been proposed for 2-AG formation (Fig. 8) starting either from glycerolipids or glycerophospholipids: 1) diacylglycerol lipase (DGL)-mediated hydrolysis of 1-acyl,2-arachidonoyl-DAGs (Fig. 11) [75]; 2) lyso-PLC-mediated hydrolysis of arachidonoyl-containing lysophospholipids (e.g. 2-arachidonoyl phosphatidylcholine) [74]; and 3) phosphatase-mediated hydrolysis of 2-arachidonoyl-lysophosphatidic acid (LPA) [71]. LPA may derive either from the PLA<sub>1</sub>-mediated hydrolysis of PA or the direct hydrolysis of lysophospholipids by a lyso-PLD. The relative importance of each of these routes to the biosynthesis of 2-AG (Fig. 11) is currently under investigation.

#### 4.3. 2-AG degradation

2-AG is rapidly internalized by neuronal cells, and, after uptake, is cleaved by serine hydrolases to generate free arachidonic acid and glycerol. Approximately 85% of the 2-AG-hydrolyzing activity in the murine brain is accounted for by monoacylglycerol lipase (MGL) [76-78]. The remaining activity has been ascribed to  $\alpha/\beta$  hydrolase-6 (ABHD-6) and  $\alpha/\beta$  hydrolase-12 (ABHD-12) [76]. Notably, because 2-AG levels are in the order of nmoles per gram of tissue in most biological tissues, its hydrolysis can provide a significant source of arachidonic acid and eicosanoids (Fig. 8) [15,73].

#### 4.4. Oxidative metabolism

As for anandamide, 2-AG can be metabolized by oxidative enzymes as effectively as arachidonic acid. LOXs-, COX-2-, and CYP450-mediated 2-AG oxygenation provides hydroxyperoxy, hydroxy, prostaglandin and epoxide metabolites (Fig. 8) [47,79-81]. Notably, because of the high physiological concentrations of 2-AG, the oxidative metabolism of this endocannabinoid may be physiologically relevant, and may give rise to a novel class of signal mediators [82,83]. For example, 2-(14,15-epoxyeicosatrienoyl)-glycerol, which is a 2-AG metabolite produced through action of CYP450, has been shown to bind with high affinity to cannabinoid receptors and exerts mitogenic activity [84]. Moreover, the hydrolysis of oxygenated derivatives of 2-AG could contribute to the mobilization of other eicosanoids (i.e. prostaglandin, hydroxy and epoxide derivatives of arachidonic acid) [45,46,82].

#### 4.5. Anabolic metabolism

2-AG can be converted into complex lipids by anabolic enzymes such as MAG kinases or acyltransferases, which generate 2-arachidonoyl-LPA and DAG, respectively. These lipids can be further converted into glycerophospholipids (through the cytidine diphosphate-DAG pathway) or TAG (Fig. 8).



#### 4.6. Ether and esters of glycerol

2-AG analogs include both cannabimimetic and non-cannabimimetic molecules.

**4.6.1. Cannabimimetic analogs**—2-Arachidonoyl glyceryl-ether or noladin ether is a metabolically stable analog of 2-AG that binds to cannabinoid receptors with high affinity [85]. This lipid was found in brain extracts, but this finding was later called into question [86,87].

**4.6.2. Non-cannabimimetic analogs**—2-AG biosynthesis is accompanied by formation of various 2-acylglycerol esters such as 2-oleoyl-*sn*-glycerol and 2-linoleyl-*sn*-glycerol [15]. Although these molecules show no distinct activity at cannabinoid receptors, they might potentiate the activity of 2-AG by reducing its lipase-mediated hydrolysis [88].

#### 4.7. Assays for the metabolism of 2-AG

Enzymatic assays of 2-AG metabolism that use fast and ultra-fast LC/MS analysis are reviewed below [15,89].

**4.7.1. DAG hydrolysis [15]**—DAG hydrolysis (e.g., by DGL activity) can be measured by incubating (at 37°C in 50 mM Tris-HCl, pH 7.0, containing 0.1% Triton X-100) a protein preparation and synthetic diheptadecanoin as substrate. The final product, monoheptanoyl glycerol, can be monitored by LC/MS using dg-2AG as internal standard.

**4.7.2. 2-AG hydrolysis [89]**—2-AG hydrolysis (e.g., by MGL activity) can be measured by incubating (at 37 °C in 50mM Tris-HCl buffer, pH 8.0 containing 0.05% bovine serum albumin) a protein preparation and 2-oleoyl-*sn*-glycerol as substrate. The final product, oleic acid, can be monitored by LC/MS using heptadecanoic acid as internal standard.

### 5. Conclusions

The use of LC/MS-based lipidomic approaches is leading to a better understanding of the interconnected lipid pathways that regulate endocannabinoid metabolism. Many questions still remain on the regulation of the biosynthesis and degradation of endocannabinoids. It can be assumed that the endocannabinoid field will greatly benefit from the development of new technologies and applications for the analysis of lipids.

### Acknowledgments

The contribution of the Agilent Technologies/University of California Irvine Analytical Discovery Facility, Center for Drug Discovery, the Agilent Technologies Foundation, Advanced Chemistry Development, Inc., the Institute for Brain Aging & Dementia and the UC Irvine Alzheimer's Disease Research Center is gratefully acknowledged. The authors would like also to thank Dr Faizy Ahmed for the numerous discussions and invaluable advices on chromatography. This work was supported by grants from the National Institute of Health (R21DA-022702, R01DK-073955, R01 DA-012413, R01DA-012447, RR274-297/3504008, RR274-305/3505998, 1RL1AA017538 to D.P. and UCI ADRC P50 AG16573).

### References

1. Katona I, Freund TF. *Nat Med* 2008;14:923. [PubMed: 18776886]
2. Di Marzo V. *Nat Rev Drug Discov* 2008;7:438. [PubMed: 18446159]
3. Piomelli D, Astarita G, Rapaka R. *Nat Rev Neurosci* 2007;8:743. [PubMed: 17882252]
4. Devane WA, Hanus L, Breuer A, Pertwee RG, Stevenson LA, Griffin G, Gibson D, Mandelbaum A, Etinger A, Mechoulam R. *Science* 1992;258:1946. [PubMed: 1470919]

5. Okamoto Y, Morishita J, Wang J, Schmid PC, Krebsbach RJ, Schmid HH, Ueda N. *Biochem J* 2005;389:241. [PubMed: 15760304]
6. Giuffrida A, Piomelli D. *FEBS Lett* 1998;422:373. [PubMed: 9498819]
7. Giuffrida, A.; Piomelli, D. *Lipid Second Messengers*. Laychock, SG.; Rubin, RP., editors. CRC Press LLC; Boca Raton, FL: 1998. p. 113
8. Hansen HH, Hansen SH, Bjornsdottir I, Hansen HS. *J Mass Spectrom* 1999;34:761. [PubMed: 10407361]
9. Schreiber D, Harlfinger S, Nolden BM, Gerth CW, Jaehde U, Schomig E, Klosterkötter J, Giuffrida A, Astarita G, Piomelli D, Markus Leweke F. *Anal Biochem* 2007;361:162. [PubMed: 17196922]
10. Williams J, Wood J, Pandarinathan L, Karanian DA, Bahr BA, Vouros P, Makriyannis A. *Anal Chem* 2007;79:5582. [PubMed: 17600384]
11. Lam PMW, Marczylo TH, El-Talatini M, Finney M, Nallendran V, Taylor AH, Konje JC. *Analytical Biochemistry*. 2008
12. Astarita G, Ahmed F, Piomelli D. *J Lipid Res* 2008;49:48. [PubMed: 17957091]
13. Weber A, Ni J, Ling KHJ, Acheampong A, Tang-Liu DDS, Burk R, Cravatt BF, Woodward D. *Journal of Lipid Research* 2004;45:757. [PubMed: 14729864]
14. Fu J, Astarita G, Gaetani S, Kim J, Cravatt BF, Mackie K, Piomelli D. *J Biol Chem* 2007;282:1518. [PubMed: 17121838]
15. Jung KM, Astarita G, Zhu C, Wallace M, Mackie K, Piomelli D. *Mol Pharmacol* 2007;72:612. [PubMed: 17584991]
16. Marczylo TH, Lam PM, Nallendran V, Taylor AH, Konje JC. *Anal Biochem* 2009;384:106. [PubMed: 18823934]
17. Kingsley PJ, Marnett LJ. *Lipidomics and Bioactive Lipids: Specialized Analytical Methods and Lipids in Disease*. 2007
18. Wakelam MJ, Pettitt TR, Postle AD. *Methods Enzymol* 2007;432:233. [PubMed: 17954220]
19. Christie, WW. *Advances in lipid methodology—Two*. Dundee: Oily Press; 1993. p. 195
20. Schmid P, Calvert J, Steiner R. *Physiol Chem Phys* 1973;5:157.
21. Bjerve KS, Daae LNW, Bremer J. *Analytical Biochemistry* 1974;58:238. [PubMed: 4825376]
22. Radin NS. *Methods Enzymol* 1981;72:5. [PubMed: 7311848]
23. Hara A, Radin NS. *Analytical Biochemistry* 1978;90:420. [PubMed: 727482]
24. Carlson LA. *Clinica chimica acta* 1985;149:89.
25. Matyash V, Liebisch G, Kurzchalia TV, Shevchenko A, Schwudke D. *The Journal of Lipid Research* 2008;49:1137.
26. Folch J, Lees M, Stanley GHS. *Journal of Biological Chemistry* 1957;226:497. [PubMed: 13428781]
27. Wenk MR, Lucast L, Di Paolo G, Romanelli AJ, Suchy SF, Nussbaum RL, Cline GW, Shulman GI, McMurray W, De Camilli P. *Nat Biotechnol* 2003;21:813. [PubMed: 12808461]
28. Cadas H, di Tomaso E, Piomelli D. *J Neurosci* 1997;17:1226. [PubMed: 9006968]
29. Cadas H, Gaillet S, Beltramo M, Venance L, Piomelli D. *J Neurosci* 1996;16:3934. [PubMed: 8656287]
30. Cadas H, Schinelli S, Piomelli D. *J Lipid Mediat Cell Signal* 1996;14:63. [PubMed: 8906547]
31. Wang J, Okamoto Y, Morishita J, Tsuboi K, Miyatake A, Ueda N. *J Biol Chem* 2006;281:12325. [PubMed: 16527816]
32. Simon GM, Cravatt BF. *J Biol Chem* 2006;281:26465. [PubMed: 16818490]
33. Leung D, Saghatelian A, Simon GM, Cravatt BF. *Biochemistry* 2006;45:4720. [PubMed: 16605240]
34. Sun YX, Tsuboi K, Okamoto Y, Tonai T, Murakami M, Kudo I, Ueda N. *Biochem J* 2004;Pt
35. Liu J, Wang L, Harvey-White J, Huang BX, Kim HY, Luquet S, Palmiter RD, Krystal G, Rai R, Mahadevan A, Razdan RK, Kunos G. *Neuropharmacology*. 2007
36. Liu J, Wang L, Harvey-White J, Osei-Hyiaman D, Razdan R, Gong Q, Chan AC, Zhou Z, Huang BX, Kim HY, Kunos G. *Proc Natl Acad Sci U S A* 2006;103:13345. [PubMed: 16938887]
37. Piomelli D. *Nat Rev Neurosci* 2003;4:873. [PubMed: 14595399]

38. Piomelli D, Beltramo M, Glasnapp S, Lin SY, Goutopoulos A, Xie XQ, Makriyannis A. *Proc Natl Acad Sci U S A* 1999;96:5802. [PubMed: 10318965]
39. Beltramo M, Stella N, Calignano A, Lin SY, Makriyannis A, Piomelli D. *Science* 1997;277:1094. [PubMed: 9262477]
40. Cravatt BF, Giang DK, Mayfield SP, Boger DL, Lerner RA, Gilula NB. *Nature* 1996;384:83. [PubMed: 8900284]
41. Wei BQ, Mikkelsen TS, McKinney MK, Lander ES, Cravatt BF. *J Biol Chem* 2006;281:36569. [PubMed: 17015445]
42. McKinney MK, Cravatt BF. *Annu Rev Biochem* 2005;74:411. [PubMed: 15952893]
43. Want EJ, Cravatt BF, Siuzdak G. *Chembiochem* 2005;6:1941. [PubMed: 16206229]
44. Saghatelian A, Trauger SA, Want EJ, Hawkins EG, Siuzdak G, Cravatt BF. *Biochemistry* 2004;43:14332. [PubMed: 15533037]
45. Kozak KR, Crews BC, Morrow JD, Wang LH, Ma YH, Weinander R, Jakobsson PJ, Marnett LJ. *Journal of Biological Chemistry* 2002;277:44877. [PubMed: 12244105]
46. Kozak KR, Crews BC, Ray JL, Tai HH, Morrow JD, Marnett LJ. *Journal of Biological Chemistry* 2001;276:36993. [PubMed: 11447235]
47. Kozak KR, Prusakiewicz JJ, Marnett LJ. *Current Pharmaceutical Design* 2004;10:659. [PubMed: 14965328]
48. Snider NT, Sikora MJ, Sridar C, Feuerstein TJ, Rae JM, Hollenberg PF. *Journal of Pharmacology and Experimental Therapeutics*. 2008
49. Hampson AJ, Hill WA, Zan-Phillips M, Makriyannis A, Leung E, Eglen RM, Bornheim LM. *Biochim Biophys Acta* 1995;1259:173. [PubMed: 7488638]
50. Fowler CJ. *British Journal of Pharmacology* 2007;152:594. [PubMed: 17618306]
51. Snider NT, Kornilov AM, Kent UM, Hollenberg PF. *Journal of Pharmacology and Experimental Therapeutics* 2007;321:590. [PubMed: 17272674]
52. Ueda N, Yamamoto K, Yamamoto S, Tokunaga T, Shirakawa E, Shinkai H, Ogawa M, Sato T, Kudo I, Inoue K, et al. *Biochim Biophys Acta* 1995;1254:127. [PubMed: 7827116]
53. Hanus L, Gopher A, Almog S, Mechoulam R. *J Med Chem* 1993;36:3032. [PubMed: 8411021]
54. Felder CC, Joyce KE, Briley EM, Mansouri J, Mackie K, Blond O, Lai Y, Ma AL, Mitchell RL. *Molecular Pharmacology* 1995;48:443. [PubMed: 7565624]
55. Farrell EK, Merkler DJ. *Drug Discovery Today* 2008;13:558. [PubMed: 18598910]
56. Schwartz GJ, Fu J, Astarita G, Li X, Gaetani S, Campolongo P, Cuomo V, Piomelli D. *Cell Metab* 2008;8:281. [PubMed: 18840358]
57. Astarita G, Di Giacomo B, Gaetani S, Oveisi F, Compton TR, Rivara S, Tarzia G, Mor M, Piomelli D. *J Pharmacol Exp Ther* 2006;318:563. [PubMed: 16702440]
58. LoVerme J, Russo R, La Rana G, Fu J, Farthing J, Mattace-Raso G, Meli R, Hohmann A, Calignano A, Piomelli D. *J Pharmacol Exp Ther* 2006;319:1051. [PubMed: 16997973]
59. Lo Verme J, Fu J, Astarita G, La Rana G, Russo R, Calignano A, Piomelli D. *Mol Pharmacol* 2005;67:15. [PubMed: 15465922]
60. Fu J, Gaetani S, Oveisi F, Lo Verme J, Serrano A, Rodriguez de Fonseca F, Rosengarth A, Luecke H, Di Giacomo B, Tarzia G, Piomelli D. *Nature* 2003;425:90. [PubMed: 12955147]
61. Maccarrone M, Cartoni A, Parolaro D, Margonelli A, Massi P, Bari M, Battista N, Finazzi-Agrò A. *Molecular and Cellular Neuroscience* 2002;21:126. [PubMed: 12359156]
62. Terrazzino S, Berto F, Carbonare MD, Fabris M, Guiotto A, Bernardini D, Leon A. *FASEB J* 2004;18:1580. [PubMed: 15289450]
63. Dalle Carbonare M, Del Giudice E, Stecca A, Colavito D, Fabris M, D'Arrigo A, Bernardini D, Dam M, Leon A. *Journal of Neuroendocrinology* 2008;20:26. [PubMed: 18426496]
64. Astarita G, Rourke BC, Andersen JB, Fu J, Kim JH, Bennett AF, Hicks JW, Piomelli D. *Am J Physiol Regul Integr Comp Physiol* 2006;290:R1407. [PubMed: 16373434]
65. Cravatt BF, Próspero-García O, Siuzdak G, Gilula NB, Heriksen SJ, Boger DL, Lerner RA. *Science* 1995;268:1506. [PubMed: 7770779]
66. Vuong LAQ, Mitchell VA, Vaughan CW. *Neuropharmacology* 2008;54:189. [PubMed: 17588618]

67. Burstein S. *Neuropharmacology*. 2007
68. McDonald GR, Hudson AL, Dunn SM, You H, Baker GB, Whittal RM, Martin JW, Jha A, Edmondson DE, Holt A. *Science* 2008;322:917. [PubMed: 18988846]
69. Jung KM, Mangieri R, Stapleton C, Kim J, Fegley D, Wallace M, Mackie K, Piomelli D. *Mol Pharmacol* 2005;68:1196. [PubMed: 16051747]
70. Bisogno T, Melck D, De Petrocellis L, Di Marzo V. *Journal of Neurochemistry* 1999;72:2113. [PubMed: 10217292]
71. Nakane S, Oka S, Arai S, Waku K, Ishima Y, Tokumura A, Sugiura T. *Arch Biochem Biophys* 2002;402:51. [PubMed: 12051682]
72. Oka S, Yanagimoto S, Ikeda S, Gokoh M, Kishimoto S, Waku K, Ishima Y, Sugiura T. *Journal of Biological Chemistry* 2005;280:18488. [PubMed: 15749716]
73. Nomura DK, Hudak CSS, Ward AM, Burston JJ, Issa RS, Fisher KJ, Abood ME, Wiley JL, Lichtman AH, Casida JE. *Bioorganic & Medicinal Chemistry Letters*. 2008
74. Sugiura T, Kishimoto S, Oka S, Gokoh M. *Progress in Lipid Research* 2006;45:405. [PubMed: 16678907]
75. Bisogno T, Howell F, Williams G, Minassi A, Cascio MG, Ligresti A, Matias I, Schiano-Moriello A, Paul P, Williams EJ, Gangadharan U, Hobbs C, Di Marzo V, Doherty P. *J Cell Biol* 2003;163:463. [PubMed: 14610053]
76. Blankman JL, Simon GM, Cravatt BF. *Chemistry & Biology* 2007;14:1347. [PubMed: 18096503]
77. Dinh TP, Kathuria S, Piomelli D. *Molecular Pharmacology* 2004;66:1260. [PubMed: 15272052]
78. Dinh TP, Carpenter D, Leslie FM, Freund TF, Katona I, Sensi SL, Kathuria S, Piomelli D. *Proc Natl Acad Sci U S A* 2002;99:10819. [PubMed: 12136125]
79. Kozak KR, Gupta RA, Moody JS, Ji C, Boeglin WE, DuBois RN, Brash AR, Marnett LJ. *J Biol Chem* 2002;15:15.
80. Moody JS, Kozak KR, Ji C, Marnett LJ. *Biochemistry* 2001;40:861. [PubMed: 11170406]
81. Kozak KR, Rowlinson SW, Marnett LJ. *J Biol Chem* 2000;275:33744. [PubMed: 10931854]
82. Kozak KR, Marnett LJ. *Prostaglandins Leukot Essent Fatty Acids* 2002;66:211. [PubMed: 12052037]
83. Woodward DF, Carling RWC, Cornell CL, Fliri HG, Martos JL, Pettit SN, Liang Y, Wang JW. *Pharmacology and Therapeutics*. 2008
84. Chen JK, Chen J, Imig JD, Wei S, Hachey DL, Guthi JS, Falck JR, Capdevila JH, Harris RC. *J Biol Chem*. 2008
85. Hanus L, Abu-Lafi S, Fride E, Breuer A, Vogel Z, Shalev DE, Kustanovich I, Mechoulam R. *Proc Natl Acad Sci U S A* 2001;98:3662. [PubMed: 11259648]
86. Fezza F, Bisogno T, Minassi A, Appendino G, Mechoulam R, Di Marzo V. *FEBS Lett* 2002;513:294. [PubMed: 11904167]
87. Oka S, Tsuchie A, Tokumura A, Muramatsu M, Suhara Y, Takayama H, Waku K, Sugiura T. *J Neurochem* 2003;85:1374. [PubMed: 12787057]
88. Ben-Shabat S, Fride E, Sheskin T, Tamiri T, Rhee MH, Vogel Z, Bisogno T, De Petrocellis L, Di Marzo V, Mechoulam R. *European Journal of Pharmacology* 1998;353:23. [PubMed: 9721036]
89. King AR, Duranti A, Tontini A, Rivara S, Rosengarth A, Clapper JR, Astarita G, Geaga JA, Luecke H, Mor M, Tarzia G, Piomelli D. *Chem Biol* 2007;14:1357. [PubMed: 18096504]
90. Larsen A, Uran S, Jacobsen PB, Skotland T. *Rapid Commun Mass Spectrom* 2001;15:2393. [PubMed: 11746908]
91. Stella N, Schweitzer P, Piomelli D. *Nature* 1997;388:773. [PubMed: 9285589]

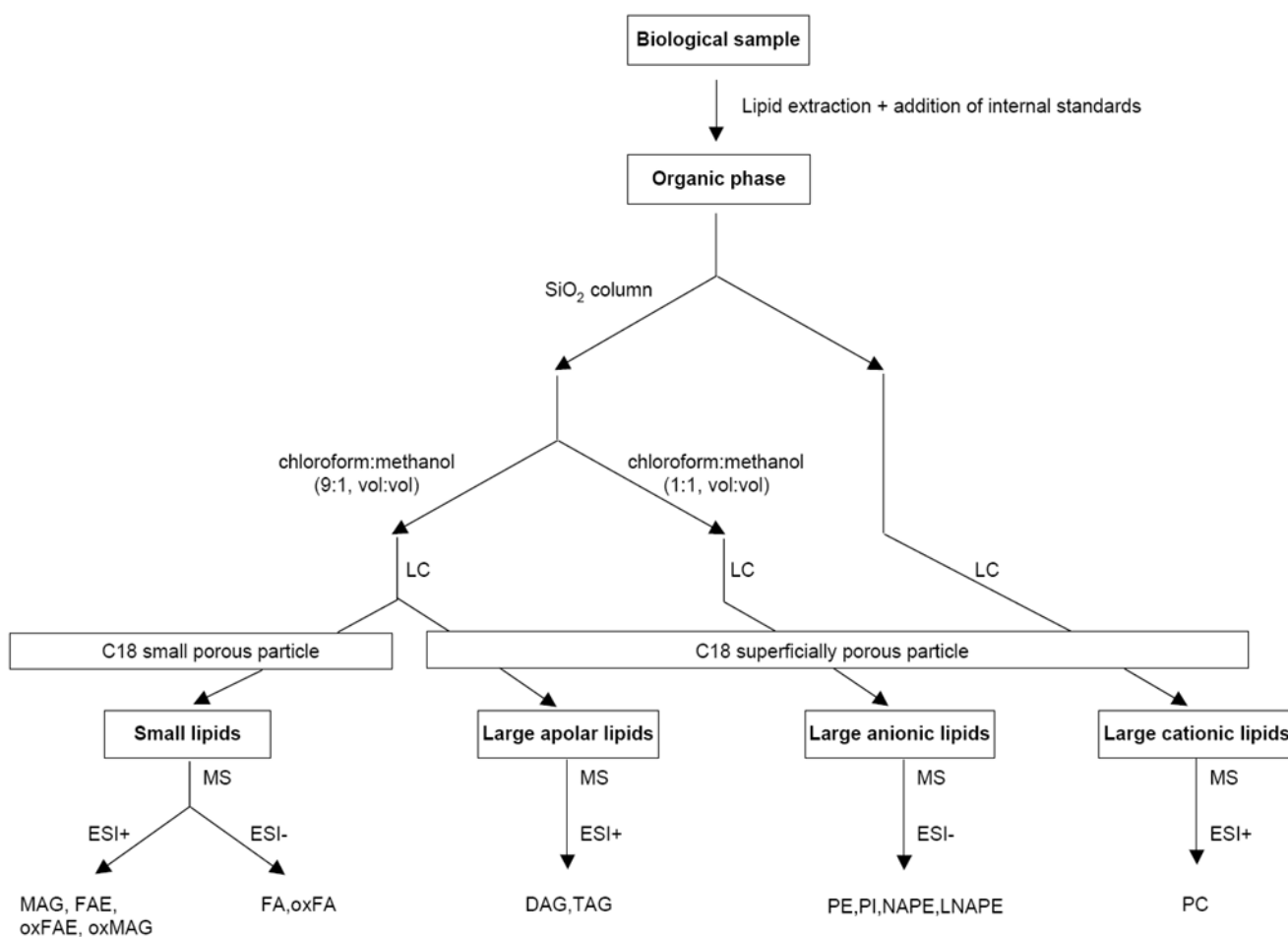


**Figure 1. Lipidomic analysis of the endocannabinoid metabolism**

Flow chart of the strategy used to profile endocannabinoid lipids from biological samples. Abbreviations: DAG, diacylglycerol; FA, fatty acid; FAE, fatty acid ethanolamide; MAG, monoacylglycerol; NAPE, *N*-acyl-phosphatidylethanolamine; LNAPE, lyso-NAPE; oxFA, oxygenated fatty acids; oxFAE, oxygenated FAE; oxMAG, oxygenated MAG; PC, phosphatidylcholine; PE, phosphatidylethanolamine; PI, phosphatidylinositol; TAG, triacylglycerol.

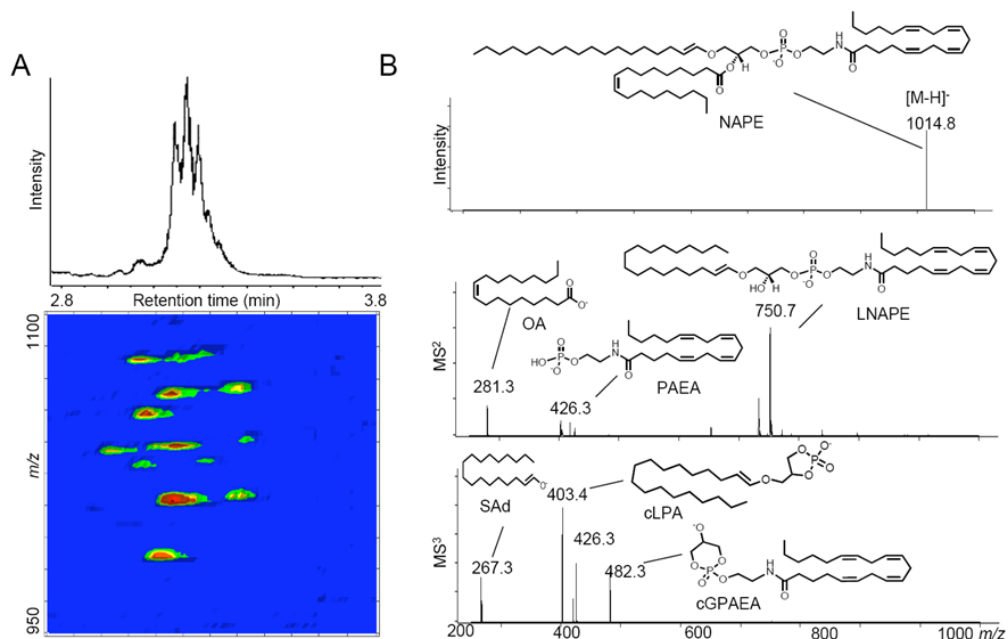


**Figure 2. LC/MS metabolite discovery tools**

A, Representative total ion LC/MS chromatogram of a mixture of isobaric and isomeric *N*-acyl phosphatidylethanolamine (NAPE) species (top). A 3D LC/MS contour mapping (bottom) visualizes individual molecular species present in the mixture. The first dimension is elution time, the second is mass-to-charge ratio ( $m/z$ ) and the third relative intensity of the signal, which is symbolized with a pseudocolor scale. LC/MS<sup>n</sup> conditions are those previously reported [12]. Three-dimensional maps were generated using MS Processor from Advanced Chemistry Development, Inc. (Toronto, Canada). B, Representative ESI/MS<sup>n</sup> analysis of *N*-arachidonoyl phosphoethanolamide species in the rat brain. MS<sup>2</sup> and MS<sup>3</sup> lead to fragment ions that are found physiologically as neutral molecular species: lyso-NAPE (LNAPE), phosphoanandamide (PAEA), oleic acid (OA), stearic aldehyde (SAd), cyclic-lysophosphatidic acid (cLPA) and a cyclic glycerophospho-anandamide (cGPAEA, which has not yet been identified in mammals).

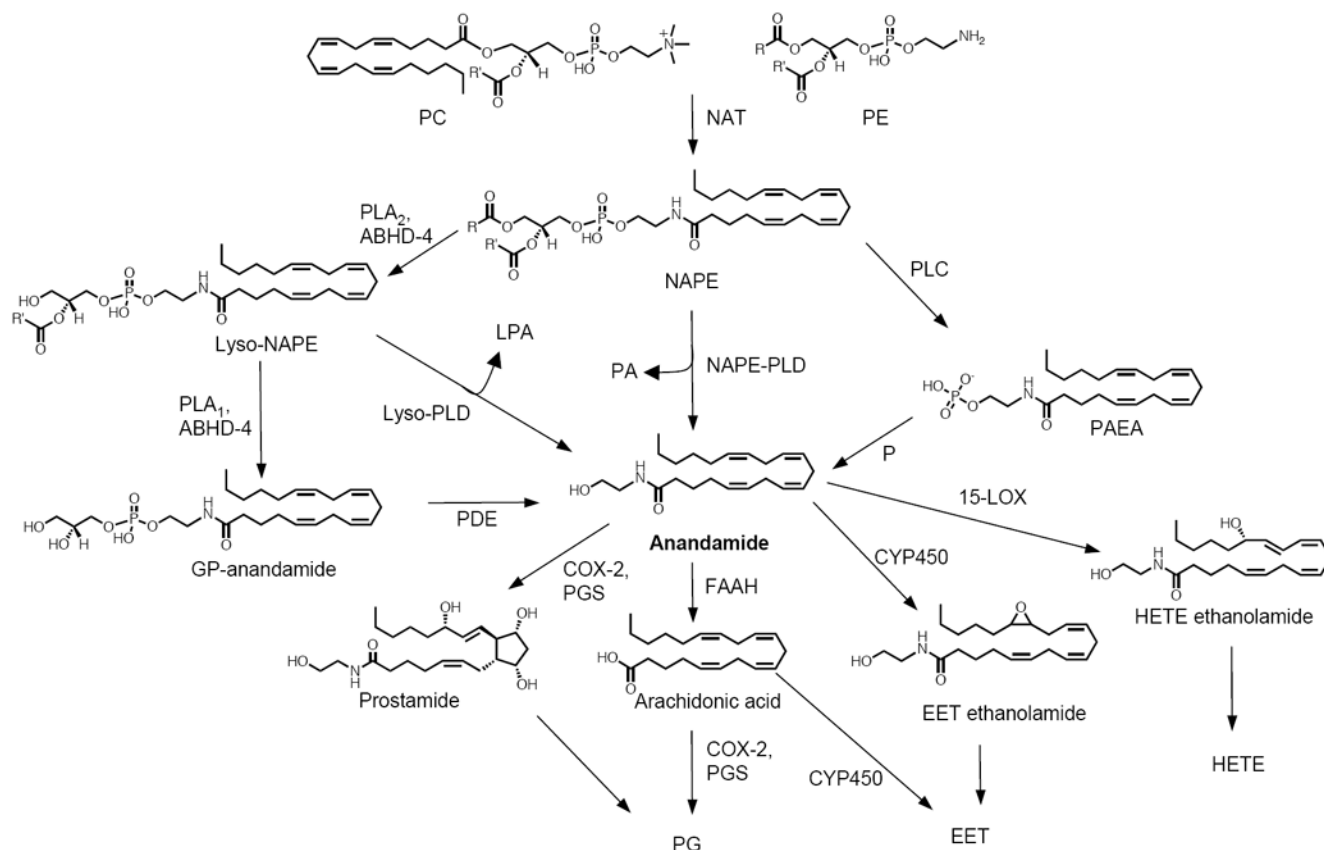


**Figure 3. Anandamide metabolism: an overview**

Postulated pathways of anandamide metabolism. Abbreviations: PC, phosphatidylcholine; PE, phosphatidylethanolamine; NAT, *N*-acyl transferase; LPA, lysophosphatidic acid; PA, phosphatidic acid; NAPE, *N*-acyl-phosphatidylethanolamine; LNAPE, 1-lyso,2-acyl-*sn*-glycero-3-phosphoethanolamine-*N*-acyl; GP-anandamide, glycerophospho-anandamide; PAEA, phosphoanandamide; PLA, phospholipase A; ABHD,  $\alpha/\beta$  hydrolase; NAPE-PLD, NAPE phospholipase D; PLC, phospholipase C; FAAH, fatty acid amide hydrolase; P, phosphatase; PG, prostaglandin; EET, epoxyeicosatrienoic acid; HETE, hydroxyeicosatetraenoic acid; COX, cyclooxygenase; PGS, prostaglandin synthase; LOX, lipoxygenase; CYP450; cytochrome P450, PDE, phosphodiesterase.

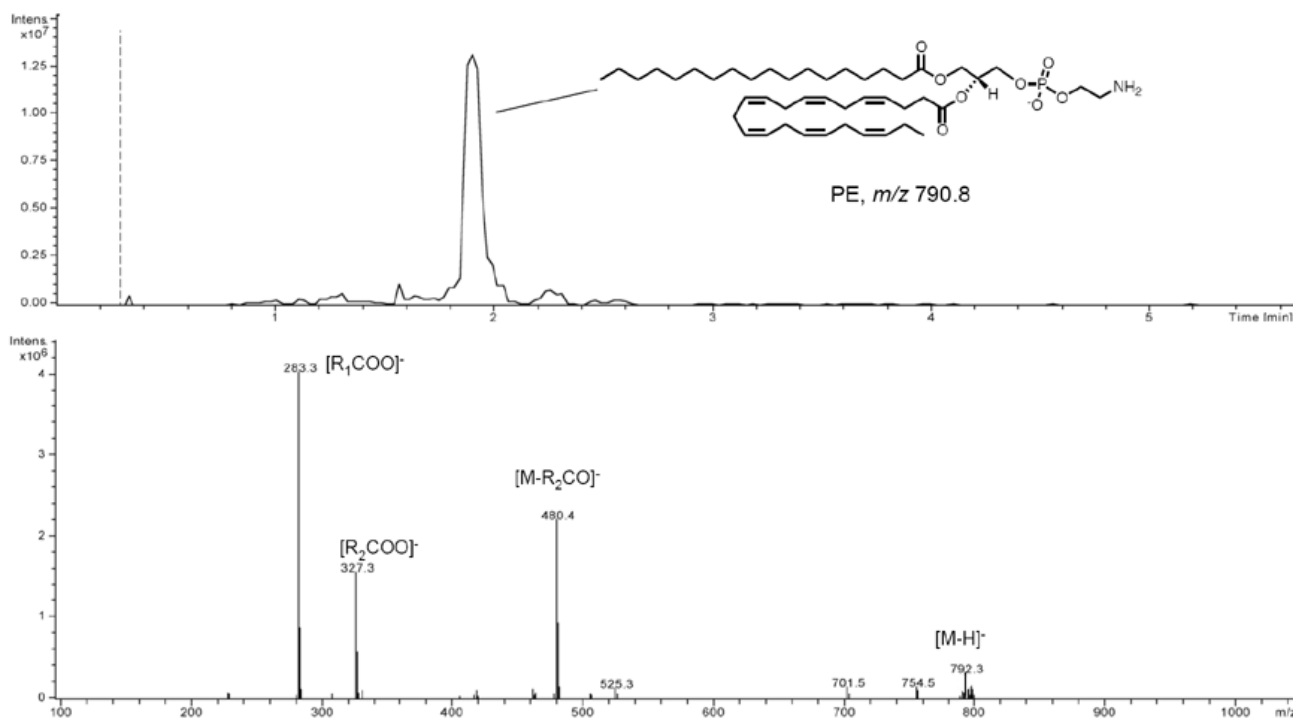


**Figure 4. Lipid remodeling and anandamide metabolism: analysis of phosphatidylethanolamine (PE) species**

Representative LC/MS analysis of PE species in a human brain. LC/MS chromatogram (top) and MS<sup>2</sup> fragmentation pattern using an ion trap mass spectrometer (bottom). PE species were detected as deprotonated molecular ions in the negative mode. In MS<sup>2</sup>, the most prominent fragments are the *sn*-2 lyso-PE in combination with the *sn*-1 and *sn*-2 carboxylate anions [90]. Sample characteristics are described in the text. Lipids were extracted from approximately 50 mg of brain tissue and resuspended in 0.1 ml of methanol. Injection volume was 10  $\mu$ l. Separation was performed on a SB300 Poroshell column (Agilent-Technologies coating layer of 0.25  $\mu$ m on total particle diameter of 5  $\mu$ m) using a linear gradient of methanol in water containing 0.25% acetic acid and 5 mM ammonium acetate (from 85% to 100% of methanol in 5 min) at a flow rate of 1.0 ml/min with column temperature set at 50  $^{\circ}$ C. Capillary voltage was 4.5kV, skimmer -40V, and capillary exit -151V. N<sub>2</sub> was used as drying gas at a flow rate of 12 liters/min, temperature of 350 $^{\circ}$ C and nebulizer pressure of 80 PSI. Helium was used as collision gas. Abbreviations: R<sub>1</sub>=*sn*-1 aliphatic chain; R<sub>2</sub>=*sn*-2 aliphatic chain.



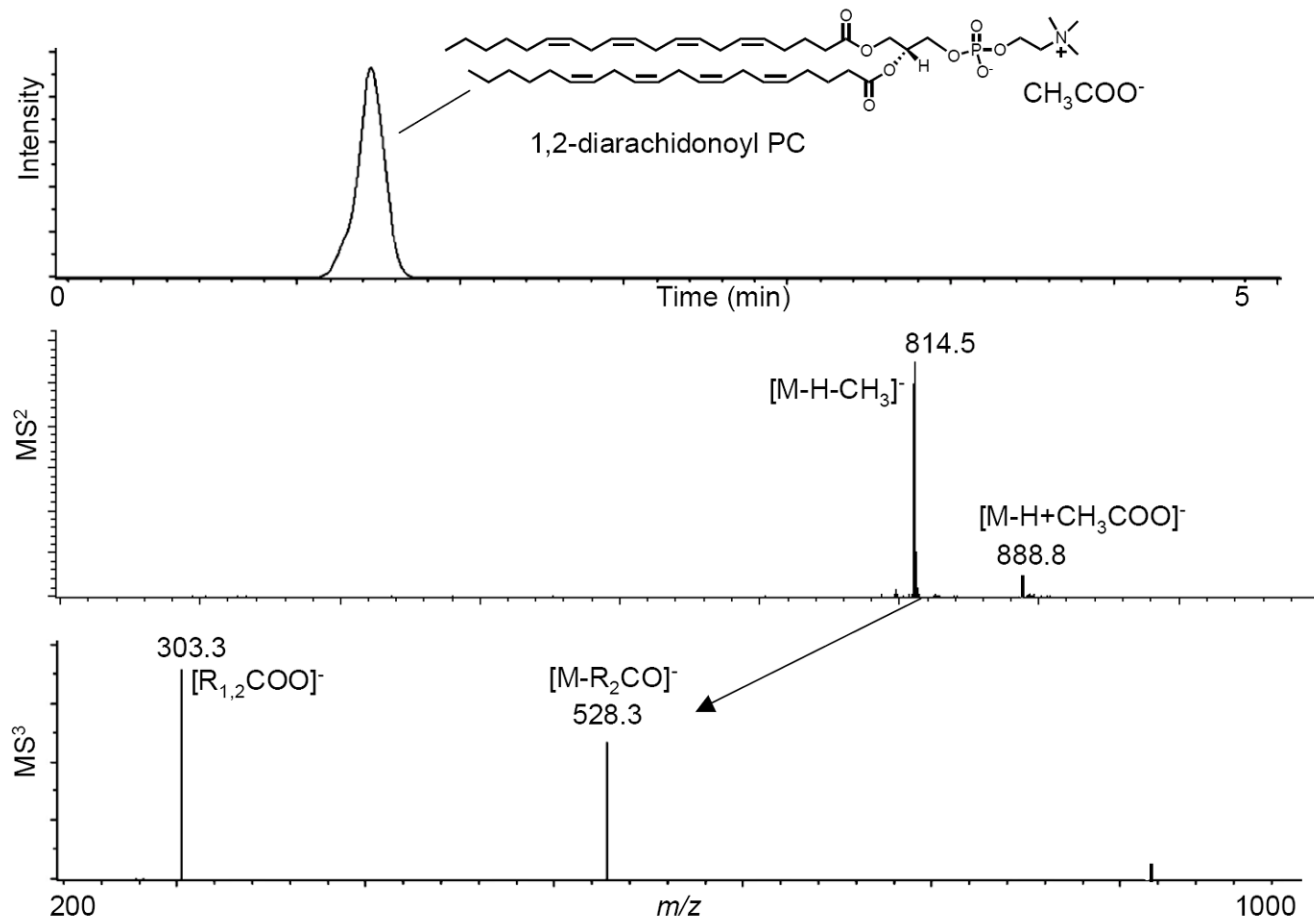


**Figure 5. Lipid remodeling and anandamide metabolism: analysis of phosphatidylcholine (PC) species**

Identification of 1,2-diarachidonoyl PC in human brain samples. LC/MS chromatogram (top) and fragmentation pattern in MS<sup>2</sup> and MS<sup>3</sup> using an ion trap instrument (bottom). Sample characteristics are described in the text and LC/MS conditions in Fig. 4 legend. Lipids were extracted from approximately 50 mg of brain tissue and resuspended in 0.1 ml of methanol. Injection volume was 10  $\mu$ l. PC species were detected as acetate adducts of the molecular ions using ESI set in the negative mode. The MS<sup>2</sup> fragmentation pattern is characterized by neutral loss of the acetate adduct of the *N*-methyl group. MS<sup>3</sup> of the ion with *m/z* 814.5 yields the lysophospholipid with neutral loss of ketene in combination with the *sn*-1 and *sn*-2 carboxylate anions. Abbreviations: R<sub>1</sub>=*sn*-1 aliphatic chain; R<sub>2</sub>=*sn*-2 aliphatic chain.

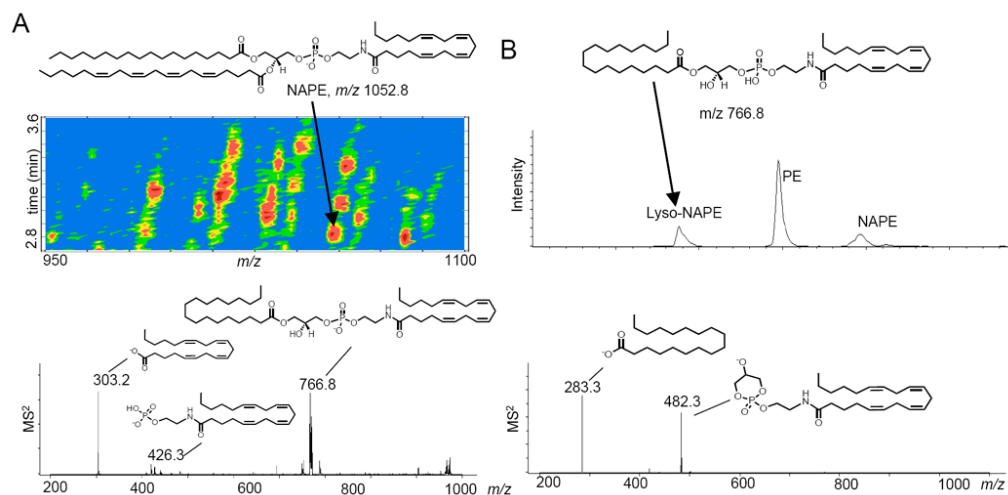


### Figure 6. Anandamide precursors: analysis of NAPE and lyso-NAPE species

Identification of endogenous NAPE (A) and lyso-NAPE species (B) in a human brain sample using LC coupled to an ion trap instrument. Sample characteristics are described in the text and LC/MS conditions in Fig. 4 legend. Lipids were extracted from approximately 50 mg of brain tissue and resuspended in 0.1 ml of methanol. Injection volume was 10  $\mu$ l. A 3D LC/MS contour mapping (A, top) of lipid extracts visualized the individual NAPE species, which were detected as deprotonated molecular ion in the negative ion mode. The first dimension is the elution time, the second is  $m/z$  ratio and the third the relative intensity of the signal, which is represented by a pseudocolor scale. In MS<sup>2</sup>, the product ions are mainly *sn*-2 lysophospholipid with neutral loss of ketene, the *sn*-2 carboxylate anion and a series of characteristic minor fragments (A, bottom) [12]. Lyso-NAPE species were separated by PE and NAPE species using the chromatographic conditions described in Fig. 4 legend (B, top). In MS<sup>2</sup>, the lyso-NAPE yielded the putative cyclic glycerophospho-anandamide and *sn*-1 carboxylate anions (B, bottom) [90].

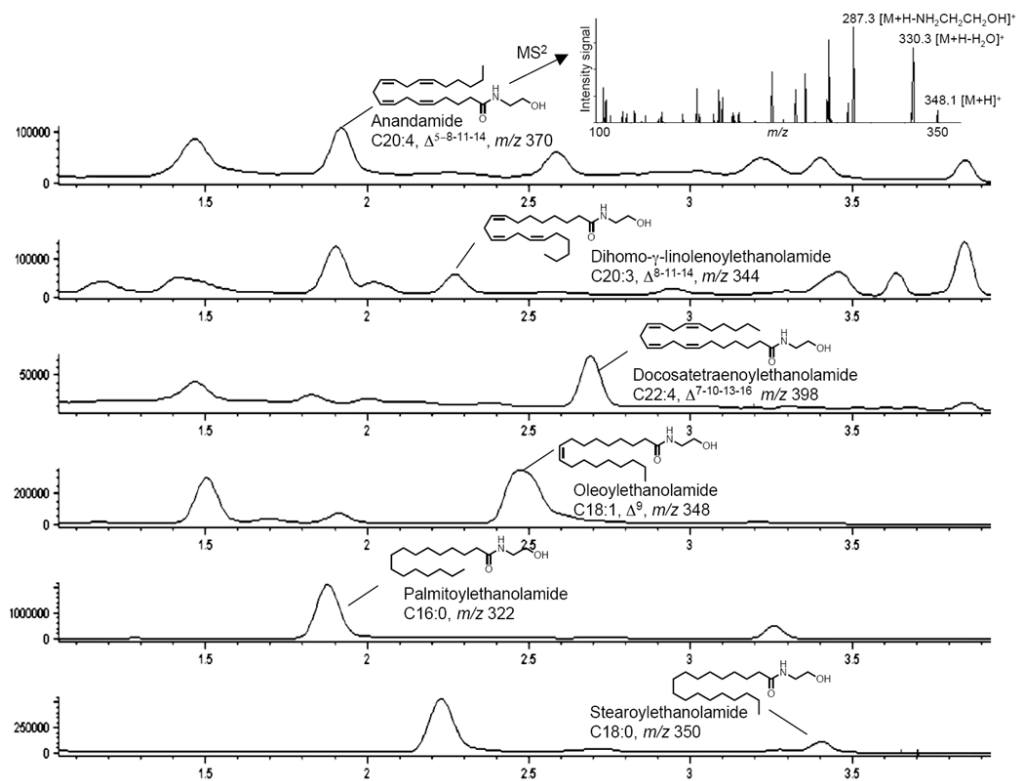


**Figure 7. Anandamide analogs: fatty acid ethanolamides (FAEs)**

LC/MS<sup>n</sup> analysis of endogenous cannabinimimetic and non-cannabinimimetic fatty acid ethanolamides (FAEs) in human brain. Sample characteristics are described in the text. Lipids were extracted from approximately 50 mg of brain tissue and resuspended in 0.1 ml of methanol. Injection volume was 10 μl. FAEs were detected as sodium adducts of the molecular ions using ESI set in the positive mode. LC/MS conditions are as described [64].





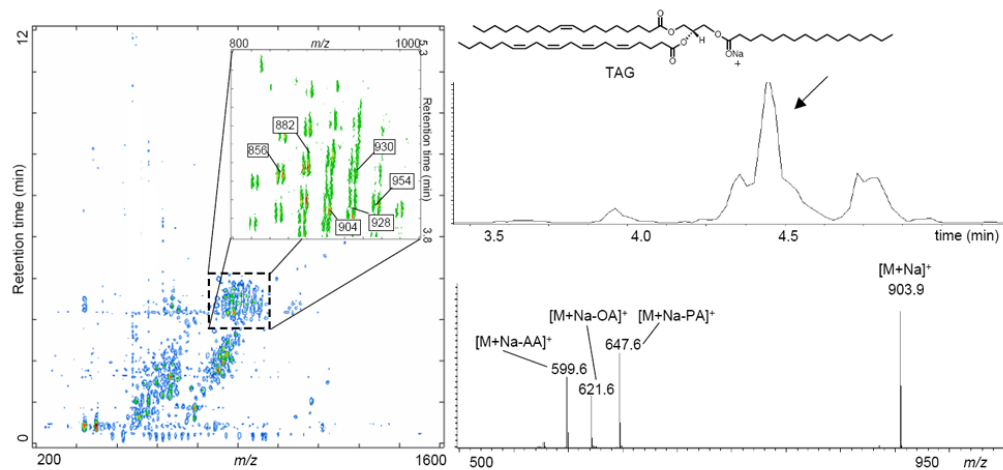


**Figure 10. Lipid remodeling and 2-AG metabolism: analysis of triacylglycerols (TAGs)**

3D representation of the TAG species present in human brain (left). Proposed structure for the arachidonoyl-containing TAG with  $m/z$  903.9 identified by LC/MS<sup>2</sup> in human brain tissue (right). LC/MS conditions are described in Fig. 4. Lipids were extracted from approximately 50 mg of brain tissue and resuspended in 0.1 ml of methanol. Injection volume was 1  $\mu$ l. TAG species were detected as sodium adducts of the molecular ions using ESI set in the positive mode. Using an ion trap instrument, MS<sup>2</sup> yielded a series of fragments deriving from the neutral loss of the *sn*-1, *sn*-2 and *sn*-3 carboxylate anions. Three-dimensional maps were generated using MS Processor from Advanced Chemistry Development, Inc. (Toronto, Canada). Abbreviations: AA, arachidonic acid; PA, palmitic acid; OA, oleic acid.

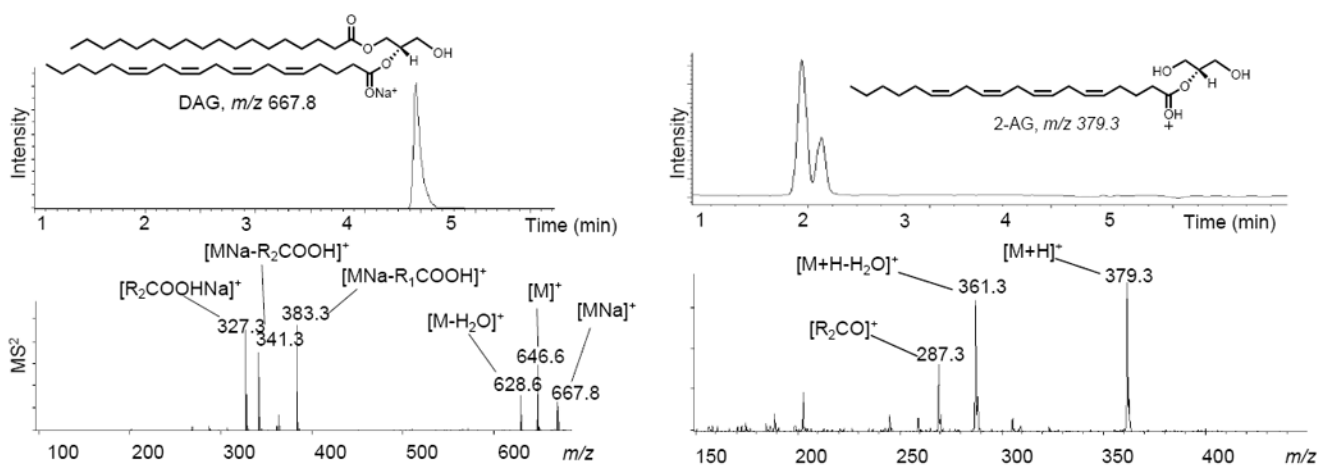


**Figure 11. 2-AG formation: analysis of DAG and 2-AG**

Representative LC/MS analysis of DAG (left) and 2-AG (right) in human brain. Lipids were extracted from approximately 50 mg of brain tissue and resuspended in 0.1 ml of methanol. Injection volume was 10  $\mu$ l. 2-AG partially isomerizes to 1-AG during extraction and is therefore detected as a double peak [91]. LC/MS conditions are those described [15]. Abbreviations:  $R_1=sn-1$  aliphatic chain;  $R_2=sn-2$  aliphatic chain.